

# **Simultaneous conventional and microwave heating for the synthesis of adsorbents for CO<sub>2</sub> capture: Comparative study to pristine technologies**

Gabriela Durán-Jiménez<sup>\*1</sup>, Jose Rodriguez<sup>1</sup>, Emily T. Kostas<sup>2</sup>, Lee A. Stevens<sup>1</sup>, Leticia Lozada-Rodriguez<sup>3</sup>, Eleanor Binner<sup>1</sup>, Chris Dodds<sup>1</sup>.

<sup>1</sup>Faculty of Engineering, the University of Nottingham, University Park, Nottingham, NG7 2RD, U.K.

<sup>2</sup>Department of Biochemical Engineering, The Advanced Centre of Biochemical Engineering, Bernard Katz Building, University College London, Gower Street, London, WC1H 6BT, U.K.

<sup>3</sup>Unidad Académica de Ciencias Químicas, Universidad Autónoma de Zacatecas, UAZ Siglo XXI, Carr. Zacatecas-Guadalajara km 6, Ejido la Escondida, Zacatecas, Zac. 98160, México

\* Corresponding author:

e-mail: gabriela.duranjimenez1@nottingham.ac.uk

Tel: +44 (0)77 2793 4248

## **Abstract**

Microwave has become an attractive technology in the valorisation of renewable biomass and in the mitigation of challenges of climate change. In this work, the synergic effects of coupling microwave and mild conventional heating conditions has been investigated in preparing engineered ultra-micropore carbons from lignocellulosic biomass. The processing conditions were systematically investigated and correlated to the physicochemical properties of activated carbons produced and their performance in post-combustion CO<sub>2</sub> capture. The highest CO<sub>2</sub> uptake (225 mg g<sup>-1</sup>) was achieved for the hybrid carbon produced at low temperature (600 °C) and modest microwave intensity. The synergic effect of hybrid heating was confirmed by the significant CO<sub>2</sub> uptake increase up to 80 and 60 % for the activated carbons prepared by microwave and conventional heating, respectively. The enhanced adsorption was confirmed by cyclic regeneration up to 99 % after 16 adsorption-desorption cycles, showing a linear correlation between the surface area, micropore volume and CO<sub>2</sub> uptake. The Pseudo-first order model accurately describes the adsorption phenomena, indicating that physisorption is the primary mechanism governing the process. The results acquired from this study highlight the process intensification in the synthesis of porous materials with comparable properties that are typically attained in conventional heating using energy intensive conditions. Additionally, this approach reveals the benefits of conventional treatment for increasing the material's microwave susceptibility and as consequence to reduce the processing time by microwave heating. The synergic effects confirms the potential of hybrid heating for applications where fast and selective heating is paramount.

**KEYWORDS:** CO<sub>2</sub> capture, simultaneous heating technologies, adsorption kinetics models, microwaves, Biomass re-utilisation, Activated carbon

## 1 Introduction

Activated carbon (AC) is one of the most versatile and utilised material used as adsorbent in the removal of textile dyes, heavy metals, pharmaceuticals from water and CO<sub>2</sub> capture. Its wide applicability is attributed to its low-cost nature, the flexible and tuneable physicochemical properties such as high porosity, large specific surface area, pH, heteroatoms content and its exceptional adsorptive capacities [1][2][3]. Its preparation using waste biomass has attracted considerable attention due to the establishment of new governmental policies around the utilisation of renewable resources to reduce the environmental impact and also to advance bio-economic aspects [4]. For many years, AC has been produced by using conventional heating methods from a series of biomasses such as agricultural wastes subjected to physical and chemical activation to increase their porosity [5]. Physical activation involves two steps where the precursor is carbonised, followed by activation with carbon dioxide or steam at high temperatures (> 850 °C). Chemical activation is a process at high temperatures which consists of the chemical impregnation of biochar in the presence of dehydrating reagents such as KOH, K<sub>2</sub>CO<sub>3</sub>, ZnCl<sub>2</sub> and H<sub>3</sub>PO<sub>4</sub> to promote pore formation by dehydration and oxidation mechanisms [6].

In many aspects, the preparation of adsorbents by conventional heating has been successfully developed to an industrial scale. This process involves the use of slow heating rate to desired final temperatures and isothermal holding (1-5 h). One of the main concerns, however, related to the use of this technology is the long processing times required to achieve the degree of activation desired, resulting in greater energy consumption [7]. New technologies are now focused on the development of methodologies that deliver improvements on the textural and chemical properties of the adsorbents, using more efficient, faster, and inexpensive processes. In the last decade, microwave heating has been widely studied as a result of its advantages,

such as unique thermal heating gradients, volumetric heating, simple, fast and its environmentally friendly technology [8][9][10]. Particularly, it has been found that microwave technology has the potential to improve processing control due to the ability to instantaneously start, accelerate the heating rate and stop the process, which is of great importance at an industrial scale [11][12][13][14].

The studied material's moisture and ionic conduction are primarily responsible for their high microwave susceptibility at lower temperatures, followed by contributions from interfacial polarisation and Joule effects at higher temperatures [15] [16] [17]. A detailed explanation of these heating mechanisms can be found in [15]. Although several investigations have shown the potential of microwave heating for the generation of high porosity in carbonaceous materials, the synergic or antagonist effects of coupling conventional and microwave technologies have been barely described [16][17]. The combination of conventional heating and microwave irradiation can be beneficial for enhancing the already known qualities of AC, that have traditionally been obtained by chemical activation using a high impregnation ratio (3:1, 6:1 chemical agent:char) [18][19] and conventional heating at high temperatures (>800 °C) and long processing times (>3 h).

The increasing carbon dioxide (CO<sub>2</sub>) concentration in the atmosphere has been recognised as the main contributor to global warming [20][21]. This in combination with the increasing global energy demand represents an urgent challenge in climate change mitigation [22][23]. In view of this, efforts associated with the transition to sustainable development and implementation of technologies for carbon capture at a large scale are mandatory. An ideal post-combustion CO<sub>2</sub> adsorbent should meet the requirements of low cost, high selectivity, and availability, efficient CO<sub>2</sub> adsorption, stability and reusability. To address these needs, in this study, we explored for the first time the synergic effects of hybrid heating combining simultaneously conventional and microwave technologies using mild processing conditions

such as low impregnation ratio, low processing temperatures and low energy, compared to conditions reported previously for the preparation of carbonaceous adsorbents. The performance of the obtained adsorbents were evaluated for post-combustion CO<sub>2</sub> adsorption. The physicochemical qualities were assessed and compared to pristine (adsorbent prepared under conventional or microwave heating) carbons produced from a sustainable waste biomass feedstock.

## **2 Materials and methods**

### **2.1 Materials**

Pecan nutshell, a lignocellulosic agricultural co-product collected from an agri-food company in México, was used as the raw material in this study. The activating agent used in this work, potassium hydroxide (KOH), was of analytical grade and purchased from Sigma-Aldrich and used without further purification. The precursor was firstly crushed and sieved to obtain a particle size ~ 0.7 mm, washed with deionised water and dried in an oven at 80 °C for 24 h, then physically mixed with KOH at mass ratio 1:1.

### **2.2 Preparation of Activated Carbons**

The AC's obtained in this work were prepared by three heating methods; conventional (C) in a Carbolite (CTF 12165/550) tubular furnace; microwave (MW) in a single-mode cavity (2 kW microwave Sairem® generator (2.45 GHz), an automatic tuner (S-TEAM STHD v1.5); and by hybrid (H) heating by coupling conventional and microwave heating. The precursor mixture with the activating agent (KOH) (8 g) was placed into an alumina vessel and introduced in the furnace using an inert atmosphere of N<sub>2</sub> at 1 L min<sup>-1</sup>. The sample was positioned 130 mm from the cavity short-circuit end (about  $\frac{3}{4}$  of the guided wavelength), using an alumina firebrick locating plate to ensure the same positioning for all tests. A schematic representation of the hybrid heating system is shown in Fig. 1.

The experimental conditions used in the preparation of adsorbents are described in Table 1. Particularly, the effect of two levels for processing time in conventional and microwave heating, and the combination of selected factors for hybrid studies were investigated. The individual temperature (conventional) and power (microwave) conditions were selected according to our previous studies which confirmed these conditions are suitable for the preparation of carbon adsorbents using single-mode cavity and conventional furnace [24] [25]. A homer auto-tuner was used in a sample to setup stubs positions to optimally deliver the power to the samples. A single-step tuning was executed at the beginning of each test resulting in high power absorption > 80% (See Fig. S1) for all tests.

The produced AC's were washed with 0.1 M HCl and deionised water until a neutral pH was obtained and dried at 105 °C in a convection oven for 24 h.

All experiments were conducted in triplicate and the data presented were obtained from the mean calculated. In general, standard deviations were below 5 % of average values.

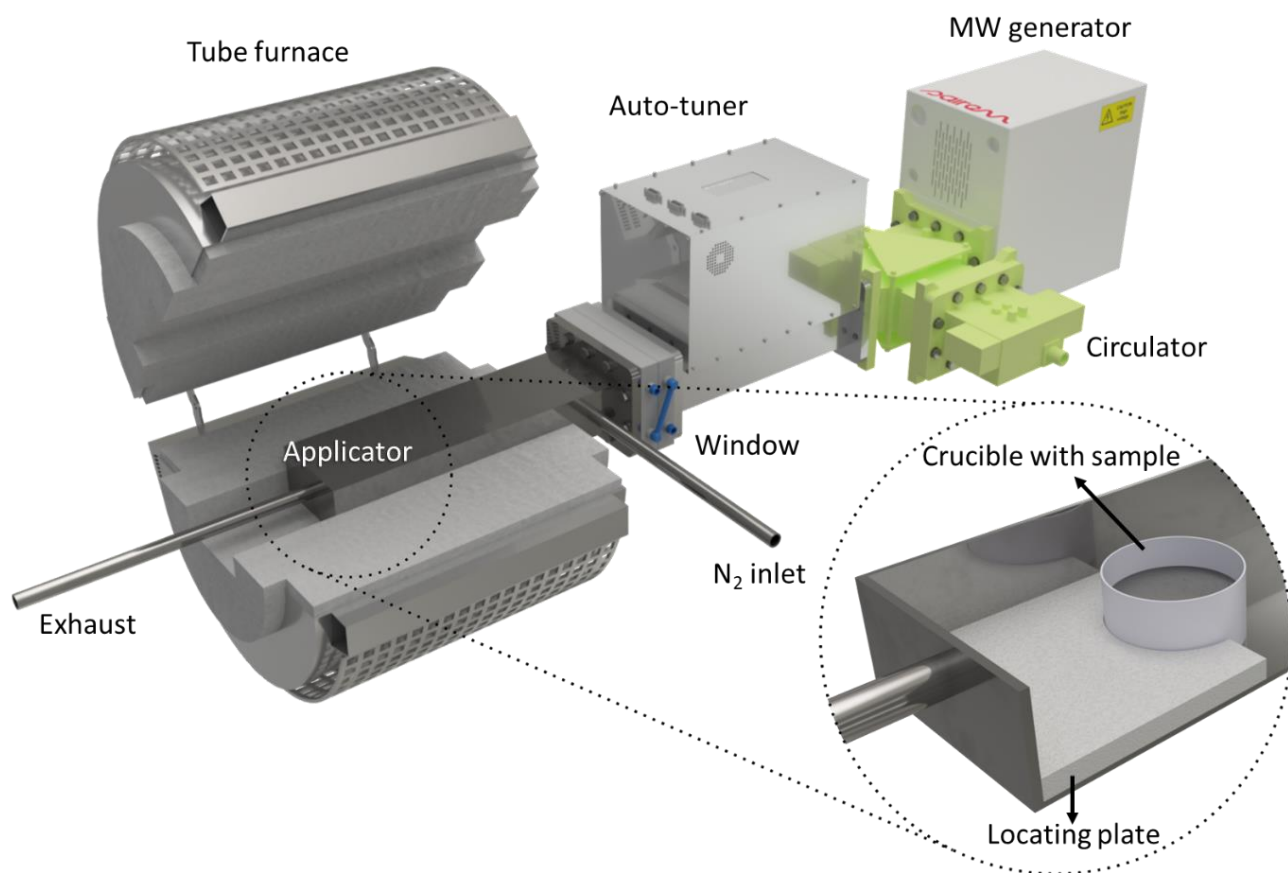


Fig. 1 System used in the synthesis of activated carbons

Table 1. Experimental conditions for the preparation of activated carbons by conventional, microwave and hybrid heating.

Sample name	Heating method	Experimental conditions
H-C60-MW8	Hybrid	Heating rate:10 °C/min, Setpoint temperature: 600 °C, time: 60 min, microwave power: 300 W, time: 8 min
H-C60-MW4	Hybrid	Heating rate:10 °C/min, Setpoint temperature: 600 °C, time: 60 min, microwave power: 300 W, time: 4 min
H-C30-MW8	Hybrid	Heating rate:10 °C/min, Setpoint temperature: 600 °C, time: 30 min, microwave power: 300 W, time: 8 min

H-C30-MW4	Hybrid	Heating rate:10 °C/min, Setpoint temperature: 600 °C, time: 30 min, microwave power: 300 W, time: 4 min
MW-8	Microwave	Input microwave power: 300 W, time: 8 min
MW-4	Microwave	Input microwave power: 300 W, time: 4 min
C-60	Conventional	Heating rate:10 °C/min, Set point temperature: 600 °C, time: 60 min
C-30	Conventional	Heating rate:10 °C /min, Setpoint temperature: 600 °C, time: 60 min

---

### 2.3 Physicochemical Characterisation of Activated Carbons

The physicochemical characterisation of the obtained AC was conducted using several analytical methods. The textural properties of the activated carbons were calculated from the sorption isotherms of N<sub>2</sub> at -196 °C using a Micromeritics ASAP 2420 apparatus. Briefly, the sample was degassed at 120 °C for 15 h to remove moisture and the surface area was calculated from the isotherm using the Brunauer–Emmett–Teller (BET) model in the P/P<sub>0</sub> range 0.01-0.04. The narrow micropore, total pore volume (up to 100 nm) and pore size distributions were determined by Non-Local Density Functional Theory (NLDFT) on carbon slit pores by combining a CO<sub>2</sub> adsorption isotherm at 0 °C to a N<sub>2</sub> adsorption isotherm beginning at 0.00001 P/P<sub>0</sub> using Microactive Software V5.0 [26].

Mid-infrared spectra were acquired using an FTIR spectrometer (Thermo Nicolet-IS10 Thermoscientific) equipped with an ATR accessory. XRD analysis was performed on a Bruker D8 Advance Da Vinci diffractometer, with 0.02° step size and step time of 10 sec in the 2θ range 10–80 °.

### 2.4 CO<sub>2</sub> uptake studies

The CO<sub>2</sub> adsorption experiments were carried out by volumetric and gravimetric analysis. The CO<sub>2</sub> uptake isotherms were obtained at 0 and 25 °C on a Micromeritics ASAP 2420 volumetric



analyser. The stability and reusability of the adsorbents was determined by gravimetric analysis using a TGA Q500 TA Instrument at 25 °C. For this test, the sample was dried at 120 °C in N<sub>2</sub> (100 mL min<sup>-1</sup>, 1 bar) for 30 min to remove the moisture. At the adsorption temperature (25 °C), the gas was switched to 100 % CO<sub>2</sub> (100 mL min<sup>-1</sup>, 1 bar) and recorded vs time for 16 adsorption-desorption cycles. For the regeneration cycles, the equilibrium time was 15 min, as defined by adsorption kinetics.

## 2.5 CO<sub>2</sub> adsorption kinetics modelling

In order to describe the adsorption behaviour, kinetic modelling was carried out on the experimental CO<sub>2</sub> adsorption kinetics for selected activated carbons (i.e. C-60, MW-8 and H-C60-MW8) using five kinetic models: Pseudo-First order, Pseudo-Second order, Elovich, Avrami and Tobin.

$$\text{Pseudo-First order} \quad \frac{dq_t}{dt} = k_1[q_e - q_t] \quad (1)$$

$$\text{Pseudo-Second order} \quad \frac{dq_t}{dt} = k_2[q_e - q_t]^2 \quad (2)$$

$$\text{Elovich} \quad \frac{dq_t}{dt} = \alpha \exp(-\beta q_t) \quad (3)$$

$$\text{Avrami} \quad q_t = q_e \{1 - \exp[-(k_A t)^{N_A}]\} \quad (4)$$

$$\text{Tobin} \quad q_t = \frac{q_e k_t t^{nt}}{1 + q_e k_t t^{nt}} \quad (5)$$

The parameters of models isotherms were determined via the global optimisation approach using a stochastic method (i.e. simulated annealing) and following the objective function [27]:

$$F_{obj} = \frac{ndat}{i=1} \sum_{i=1}^{ndat} \left( \frac{q_t^{exp} - q_t^{calc}}{q_t^{exp}} \right)_i^2 \quad (6)$$

where  $q_{exp}$  and  $q_{calc}$  are the experimental and predicted adsorption capacities, respectively. The mean absolute percentage deviation ( $E_{abs}$ ) between calculated and experimental  $CO_2$  adsorption capacities was calculated as follow:

$$E_{abs} = \frac{100}{ndat} \sum_{i=1}^{ndat} \left| \frac{q_t^{exp} - q_t^{calc}}{q_t^{exp}} \right|_i \quad (7)$$

### 3 Results and Discussion

#### 3.1 Textural properties

Some of the critical factors that influence the performance of AC for  $CO_2$  capture are the surface area, pore size and pore distribution. Fig. 2 shows the adsorption-desorption nitrogen isotherms for the AC's, which are type 1a) according to the IUPAC classification. The pronounced increase of absorbed volume at a relative pressure ( $P/P_0 < 0.1$ ) is indicative of large volume of narrow micropores [26]. The summary of textural properties is shown in Table 2. In general, it can be observed that the specific surface area increased substantially in the hybrid activated carbons, confirming the complete gasification and formation of the porous structure as a result of the coupled heating technologies. In general, the surface area increased in the following order: Conventional AC < Microwave AC < Hybrid AC. In this sense, it is important to note that the processing time positively affected the development of the porous structure. For example, the sample prepared conventionally in 60 min (C-60) showed an increase of 23% in the surface area compared to the respective at 30 min (C-30). For the samples prepared by microwave heating, a similar positive effect was observed for the sample prepared at 8 min (MW-8), with an increment up to 32% in the surface area compared to the sample prepared at 4 min (MW-4). A comparative  $S_{BET}$  area was reported in the literature ( $536 \text{ m}^2 \text{ g}^{-1}$ ) for activated carbon prepared at  $600 \text{ }^\circ\text{C}$  for 60 min in conventional heating and rice husk as a biomass precursor [28].

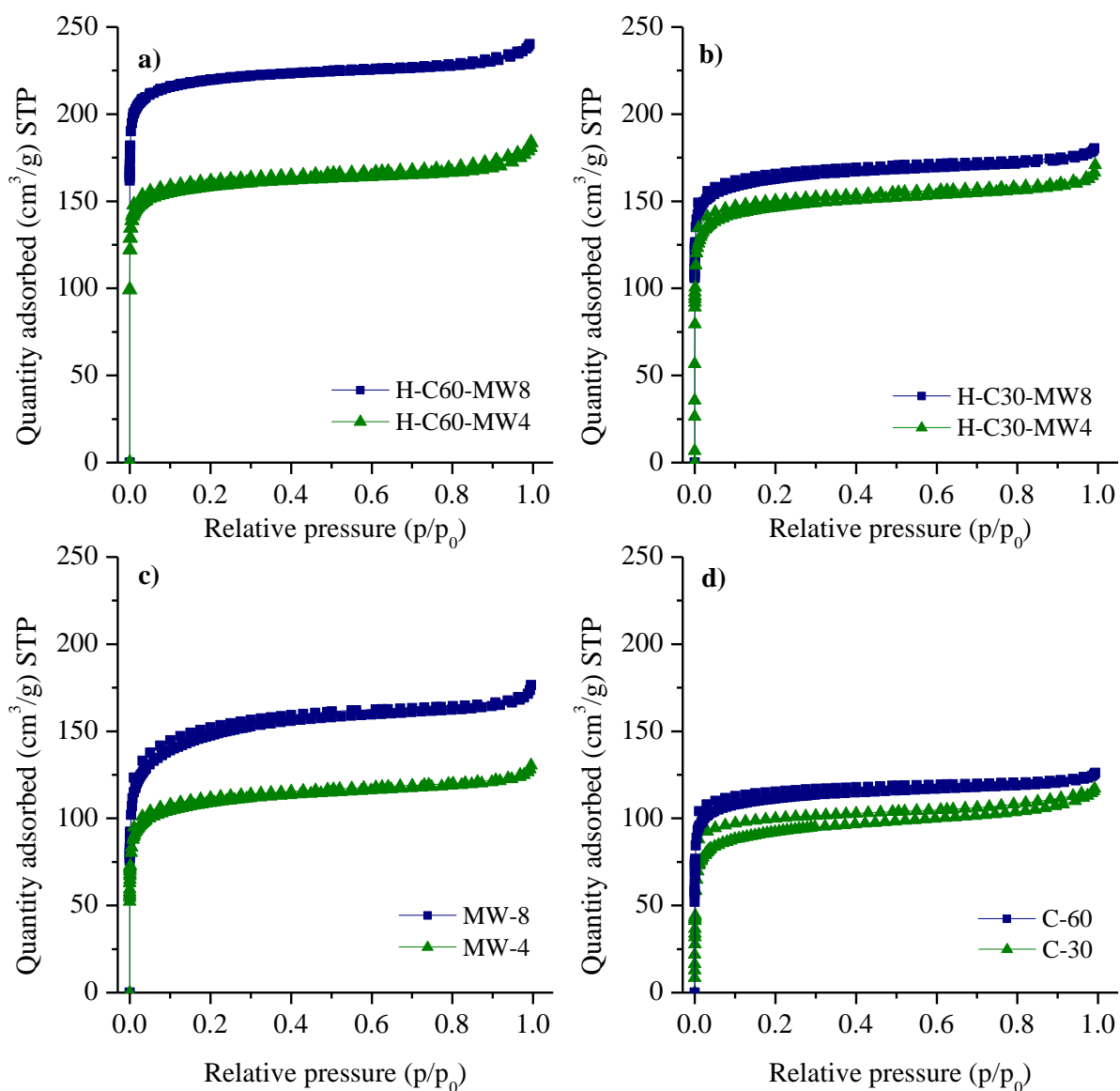


Fig.2. N<sub>2</sub> adsorption-desorption isotherms of hybrid, microwave, and conventional activated carbons

The synergic effects of coupling conventional and microwave heating are evident for all the hybrid samples compared to the pristine carbons by conventional or microwave heating. A direct correlation was established between the processing time for both heating technologies and the development of the porous matrix in the material. Interestingly, it was found that the hybrid sample prepared at 60 min of conventional heating and 8 min of microwave (H-C60-MW8) had the highest surface area (887 m<sup>2</sup> g<sup>-1</sup>), which is up to 146, 109, 100 and 58% higher

than the specific surface area shown for C30, MW-4, C-60 and MW-8, respectively. In this sense, it is worth highlighting that for the hybrid ACs the combination of microwave and conventional heating at longer processing times is highly beneficial.

Table 2. Textural parameters of AC prepared in this work

Sample	<sup>a</sup> S <sub>BET</sub> (m <sup>2</sup> /g)	<sup>b</sup> V <sub>p</sub> (cm <sup>3</sup> /g)	<sup>c</sup> V <sub>mic&lt;2nm</sub> (cm <sup>3</sup> /g)	<sup>d</sup> V <sub>&lt;0.8nm</sub> (cm <sup>3</sup> /g)
H-C60-MW8	887 ± 0.33	0.344	0.320	0.287
H-C60-MW4	638 ± 0.46	0.270	0.240	0.180
H-C30-MW8	649 ± 1.20	0.263	0.240	0.187
H-C30-MW4	584 ± 0.96	0.239	0.213	0.096
MW-8	562 ± 0.67	0.255	0.212	0.133
MW-4	425 ± 0.22	0.190	0.161	0.101
C-60	444 ± 1.10	0.184	0.164	0.097
C-30	361 ± 1.57	0.166	0.127	0.048

<sup>a</sup> Specific surface area calculated by the BET model.

<sup>b</sup> Total pore volume (up to 100 nm)

<sup>c</sup> Micropore volume obtained at 2 nm.

<sup>d</sup> Ultra-micropore volume at 0.8 nm

Fig. 3 illustrates the pore size distribution for the activated carbons prepared in this work. It can be seen that total pore volume depends on the heating mechanism and the processing time. The total pore fraction increases in the following order: H-C60-MW8 > H-C60-MW4 > H-C30-MW8 > MW-8 > H-C30-MW4 > MW-4 > C-60 > C-30. The pores with diameters in the range of ultra-micropores (<0.8 nm) appeared to increase in the carbons prepared by a combination of both conventional and microwave heating. In sample H-C60-MW8, up to 84 % of the total pore volume corresponds to pores of a diameter smaller than 0.8 nm. A significant enhancement in the micro and ultra-microporosity was observed in all hybrid carbons compared to the carbons using pristine heating technologies. For example, samples C-60 and MW-8 showed a

micropore volume of 0.184 and 0.212 cm<sup>3</sup> g<sup>-1</sup>, respectively. By combining conventional and microwave heating, the micropore volume increased up to 0.344 cm<sup>3</sup> g<sup>-1</sup> (H-C60-MW8) which represents an increase of 35 and 82%, respectively.

In Fig. 3 (c-d), it can be observed that in both pristine heating samples, the pore size distribution is well defined, showing a peak in the ultra-micropore region around 0.37 and 0.48 nm for conventional and microwave activated carbons. In hybrid activated carbons at 8 min (Fig. 3 a-b)), new peaks were identified at 0.36 and 0.51 nm. An additional peak at 0.55 nm was reported in sample H-C60-MW8. The enhanced micropore formation in the hybrid carbon could be related to complete gasification of the sample by potassium decomposition at higher temperatures. The general mechanism for pore formation starts at low temperatures, where the potassium hydroxide leads to the oxidation of the carbon, resulting in the formation of potassium carbonate that is then further reduced to hydrogen and metallic potassium. The potassium gasification induces swelling and disintegration of the carbon structure, resulting in the framework expansion and pore formation [24][29]. The reactions involved in the activation process are described below:



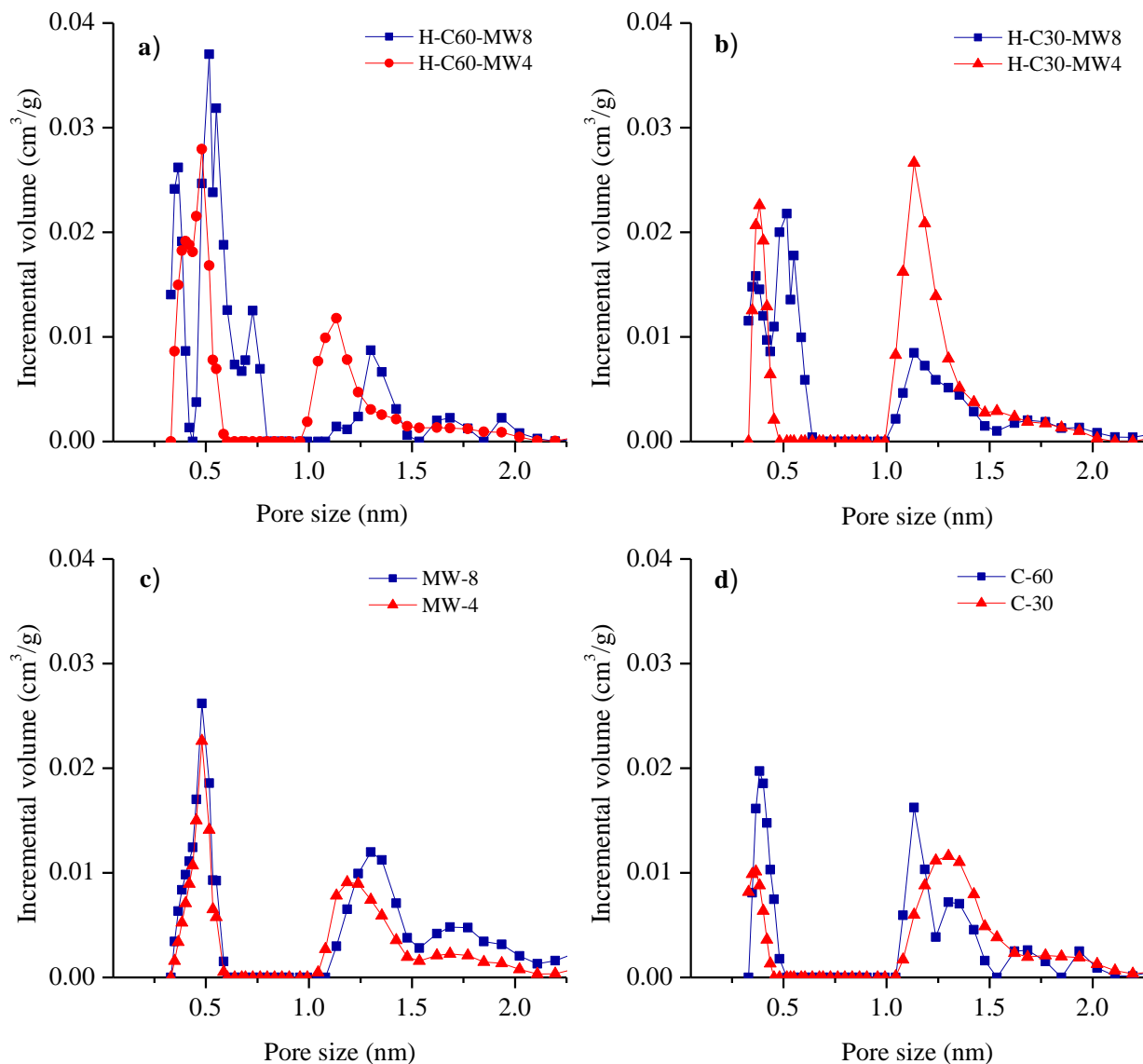


Fig. 3. Pore size distribution of activated carbon prepared in hybrid, conventional and microwave heating

### 3.2 CO<sub>2</sub> adsorption results

The CO<sub>2</sub> uptake onto the hybrid, conventional and microwave synthesized AC's in this study are shown in Table 3 & Fig.4. The highest CO<sub>2</sub> uptake was reported for the hybrid AC's followed by the microwave and conventional at 8 and 30 min, respectively. The CO<sub>2</sub> adsorption isotherms at 0 °C illustrated in Fig. 4 depict the adsorptive properties of AC's as a function of the processing time. In conventional heating, the maximum adsorption capacity was 125 mg g<sup>-1</sup>

<sup>1</sup> for the sample C-60, compared to 110 mg g<sup>-1</sup> for C-30. In microwave heating, an adsorbed amount of 143 mg g<sup>-1</sup> was reported by the sample prepared at 8 min (MW-8), up to 25% higher than the sample MW-4 (114 mg g<sup>-1</sup>). It is important to note that by comparing only microwave and conventional heating, the results indicate microwave heating is a promising technology for the synthesis of ACs for gas purification, due to the reduced processing times and end-qualities achieved.

Table 3. CO<sub>2</sub> uptake reported at 25 °C and 1 bar for AC prepared in this work

Sample	CO <sub>2</sub> uptake (mg g <sup>-1</sup> ) at 25 °C, 1 bar, 100% CO <sub>2</sub>
H-C60-MW8	146 ±0.44
H-C60-MW4	137 ±0.63
H-C30-MW8	128 ±0.72
H-C30-MW4	117 ±0.54
MW-8	97 ±0.76
MW-4	76 ±0.75
C-60	94 ±0.57
C-30	79 ±0.84

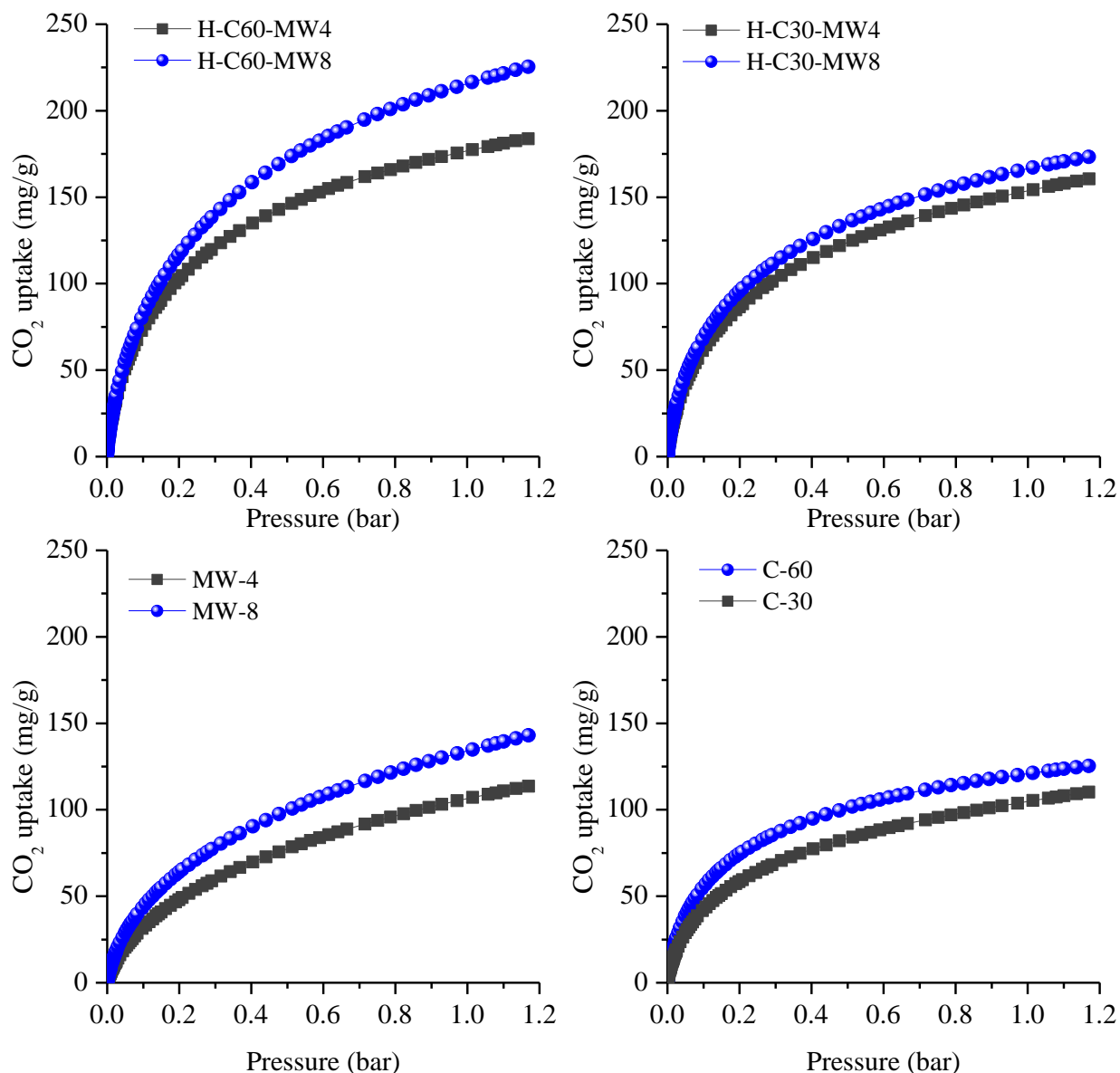


Fig.4. CO<sub>2</sub> adsorption profiles at 0 °C for conventional, microwave and hybrid activated carbons. Conditions: Volumetric method, 100% CO<sub>2</sub>.

Fig. 4 evidenced the synergic effect of combining microwave with conventional heating to increase the performance of activated carbons. In this sense, the sample H-C60-MW8 reported a maximum adsorption capacity up to 225 mg g<sup>-1</sup>. The hybrid sample prepared at 4 min (H-C60-MW4) showed a CO<sub>2</sub> uptake of 184 mg g<sup>-1</sup>. This represents an increment up to 80 and 58% compared to the pristine activated carbons C-60 and MW-8, respectively. The maximum adsorption capacity reported in this study (225 and 164 mg g<sup>-1</sup> at 0 and 25 °C, respectively. 1:1



KOH:biomass impregnation ratio) is comparable or higher than other porous materials prepared at higher temperatures  $>800\text{ }^{\circ}\text{C}$  and higher impregnation ratio such as N-enriched porous carbon materials ( $140\text{ mg g}^{-1}$ ) [30], activated carbon from palm empty fruit bunch ( $140\text{ mg g}^{-1}$ ) [18], metal-treated wood ( $83\text{ mg g}^{-1}$ ) [31], date seeds ( $129\text{ mg g}^{-1}$ ) [32] and pine nutshell activated carbon ( $220\text{ mg g}^{-1}$ ) [33], pollen derived carbons ( $77$  &  $247\text{ mg g}^{-1}$  at 1:1 & 3:1 KOH:pollen carbon ratio, respectively) [34] and date stone activated carbon ( $281\text{ mg g}^{-1}$  using an activation temperature of  $800\text{ }^{\circ}\text{C}$  and 6:1 KOH:char ratio) [35]. The  $\text{CO}_2$  uptake achieved by the materials prepared in this study showed three key benefits in hybrid heating technology:

- a) It is possible to eliminate one step in the preparation of activated carbons. Direct KOH-biomass impregnation showed the potential for the development of pore structure without the need of pre-carbonise the biomass.
- b) The  $\text{CO}_2$  adsorptive capacities of AC indicated that by using low impregnation ratio (1:1) is possible to achieve comparable  $\text{CO}_2$  uptakes in AC prepared at high impregnation ratio (6:1). This represent and economic and environmental improvement for the minimisation of chemicals and waste generated.
- c) By coupling microwave and conventional heating, is possible to reduce the processing times from 4-6 h to 1.2 h.

### **3.2.1 Correlation between physicochemical properties and the $\text{CO}_2$ uptake**

Fig. 5 shows the comparison between the hybrid activated carbons with the pristine conventional technologies. The synergic effect is notable in specific surface area ( $S_{\text{BET}}$ ) and the adsorbed amount of  $\text{CO}_2$ . Fig. 5 a) illustrates the significant improvement in both parameters when the sample is prepared by a combination of microwave heating for 8 min in conventional heating (C-60). This effect could be explained due to the longer microwave processing time (8 min). The sample achieved higher temperatures that ultimately lead to the competition of redox

reactions and generation of the porous structure [36]. It has been demonstrated that KOH/char ratio play a significant role in the development of a larger surface area, using ratios up to 5. Nevertheless, this study selected a low ratio of impregnation (KOH/biomass ratio of 1:1) to highlight only the benefits of coupling the two heating mechanisms and reduce the costs involved in the preparation of the adsorbent. Similar beneficial effects of hybrid heating were observed at lower microwave processing times (Fig. 5 c)).

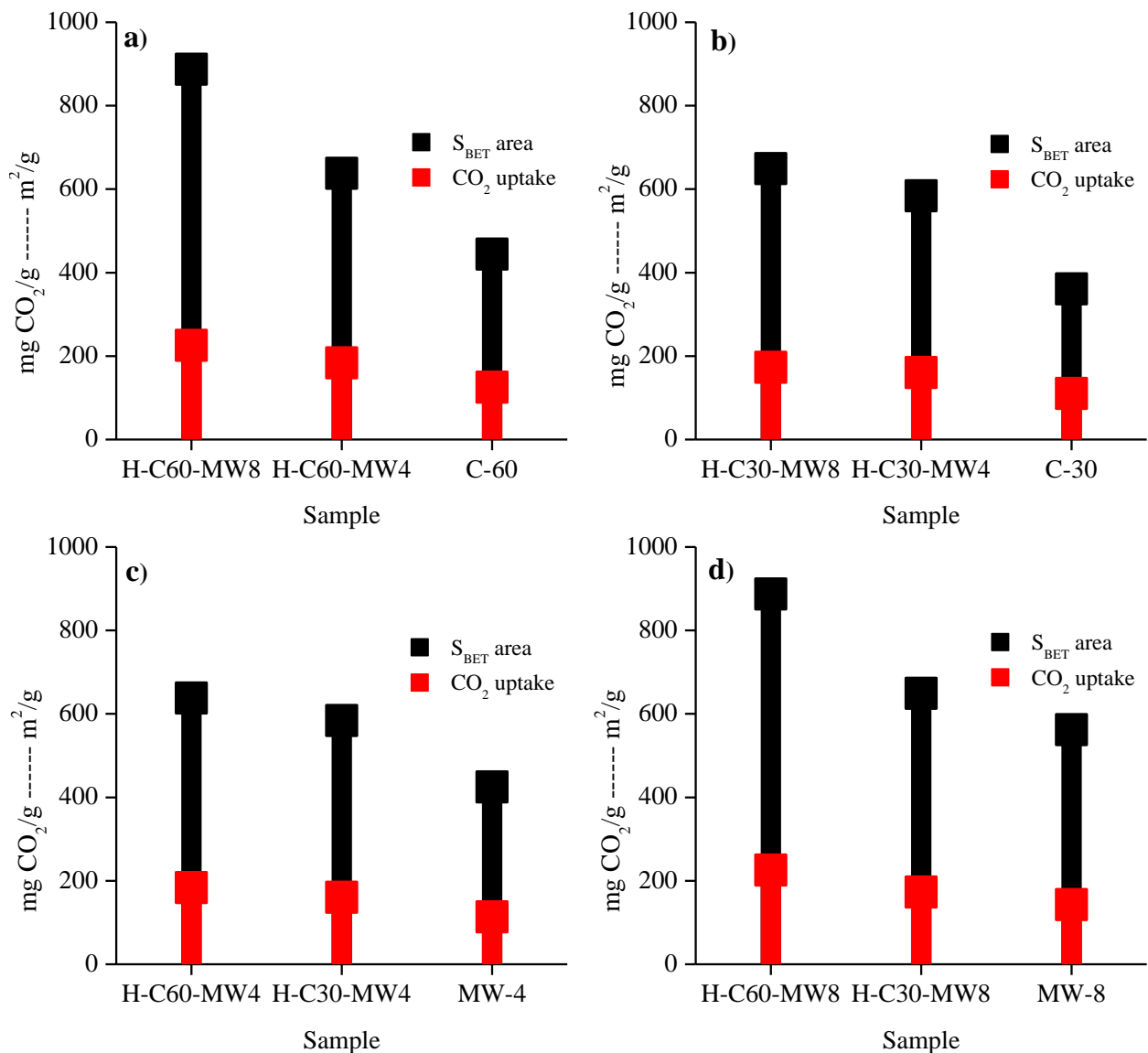


Fig. 5. Hybrid heating effect on the textural properties and CO<sub>2</sub> capture. Microwave time effect on conventional heating (a-b) and conventional time in microwave treatment (c-d)

The correlation between the micro & ultra-micropore volume, specific surface area, and total pore volume with the CO<sub>2</sub> uptake is shown in Fig. 6. The results indicate a strong linear correlation with high regression coefficient ( $R^2 > 0.96$ ) for the adsorbed amount with the specific surface area. From the total volume of pores, the best linear correlation exists between the micropore volume (<2 nm) with  $R^2 > 0.95$ . In recent studies, it has been reported that at low pressures, the micropore volume, particularly the ultra-micropores (<0.8 nm), are responsible for the enhancement of the CO<sub>2</sub> uptake [33][37], while pores with widths larger than three times the molecular diameter of the gas are negligible [38]. These results confirm that efficient CO<sub>2</sub> adsorption can be achieved for materials that pose a large amount of narrow micropores.

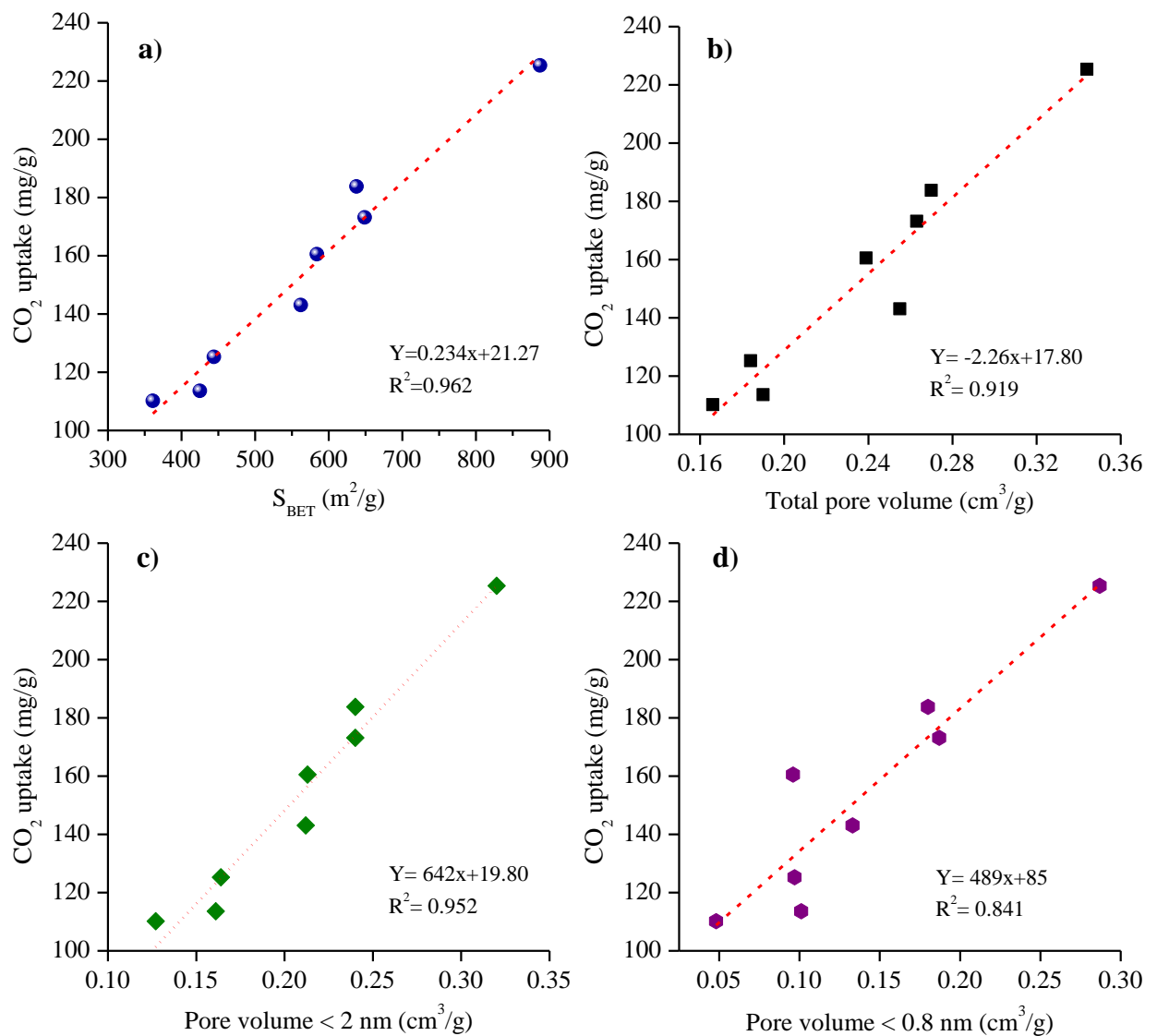


Fig. 6. Correlation between the textural properties of activated carbons and CO<sub>2</sub> adsorption

### 3.2.2 Physicochemical characterisation

In order to evaluate the creation or loss of surface functional groups of precursor and activated carbons, FT-IR analysis was conducted. The results are presented in Fig. 7 a). As expected, the peaks of modes of vibration of functional groups in the precursor disappeared gradually for activated carbons C-60, MW-8 and H-C60-MW8, respectively. The peaks shown in the precursor are characteristic of lignocellulosic biomasses; the peak at 3367 cm<sup>-1</sup> corresponds to the stretching vibration O-H of hydroxyl groups, while the peaks between 2927 and 2864 cm<sup>-1</sup> are assigned to asymmetric C-H and symmetric C-H stretching vibration of alkyl groups as methyl. The peak at 1735 cm<sup>-1</sup> could be related to carboxylic acid, while the peaks between 1508 and 1623 cm<sup>-1</sup> can be attributed to the C=C stretching vibration of aromatic structures in the activated carbons [39]. The peaks at 1184, 879 & 819 cm<sup>-1</sup> in C-60 are assigned to the C-O stretching vibration of unsaturated ethers. The distinctive band at ~1570 cm<sup>-1</sup> can be assigned to the C=C stretching vibration in alkenes [40].

The XRD diffractograms are shown in Fig. 7 b) and are characteristic of ACs displaying two prominent diffused peaks at 2θ ~23 & 43 °, which corresponds to the diffuse (002) and diffraction (100) of graphitic carbonaceous materials. The broad peak at 23 ° represents the amorphous nature, while the band at 43 ° indicates the interlayer spacing of the aromatic layers [41]. By comparing the XRD patterns of H-C60-MW8 with C-60, it is evident the diffraction peak at (002) is less broad suggesting a higher degree of graphitisation that could be a result of a complete reaction of the KOH and the biomass at higher carbonisation temperatures. The pattern indicates that the orientation of graphitic layers in the adsorbent is intimately associated with the expansion and distribution of carbon lattices resulting in the development of the high surface area and micropore structure [42].

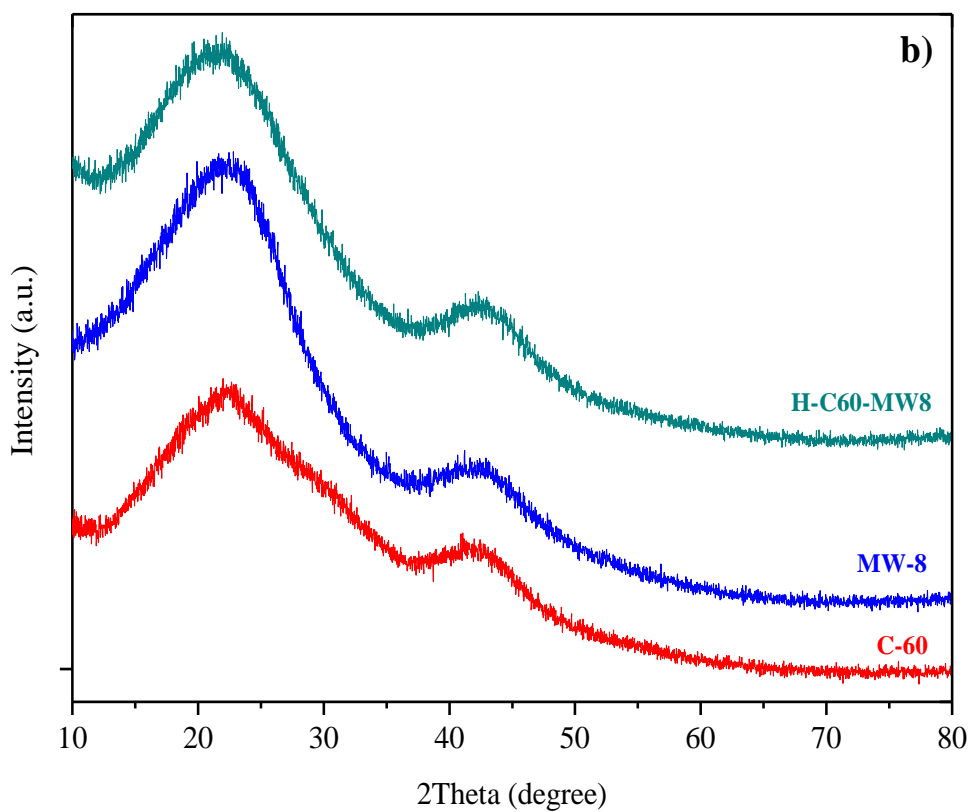
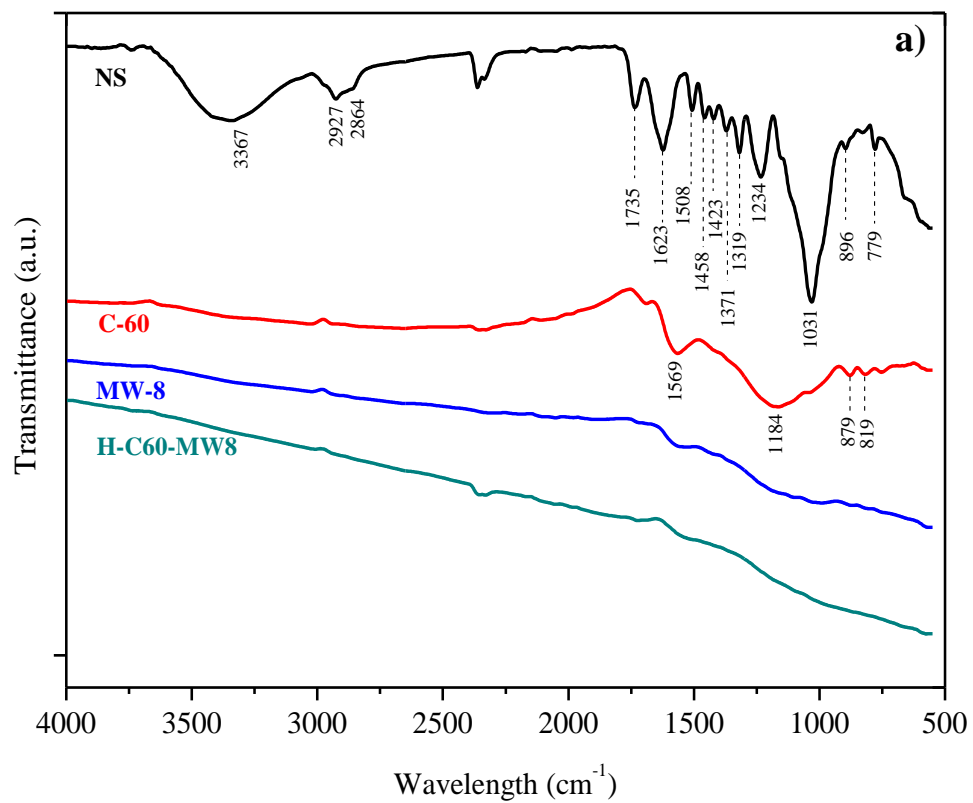


Fig.7. FT-IR spectra (a) & XRD patterns (b) of selected activated carbons prepared in this work

### 3.3 CO<sub>2</sub> adsorption Kinetics and model fitting

The assessment of the adsorption kinetics is fundamental to evaluate the adsorption suitability in industrial applications. The best combination is an adsorbent having high uptake capacity with a fast adsorption rate. In this sense, the adsorption kinetics for H-C60-MW8, MW-8 and C-60 at 25 °C and 1 bar are shown in Fig. 8 a). In general, it can be observed that the CO<sub>2</sub> was quickly absorbed in less than 2.5 min for all carbons. However, the adsorption equilibrium is first reached by the hybrid activated carbon (H-C60-MW8). This can result from its highest and homogenised surface area that could improve the mass transfer and CO<sub>2</sub> diffusion from the surface to the ultra-microporous matrix structure. Pseudo-first order, pseudo-second order, Elovich, Avrami and Tobin kinetics models were used to investigate the mechanism of the adsorption. The model and parameter fittings are shown in Fig. 8 and Table 4. It can be seen that the CO<sub>2</sub> adsorption on H-C60-MW8 and MW-8 was best fitted by the pseudo-first order kinetic model, while C-60 showed better fitting to the pseudo-second order model because of the highest correlation coefficients,  $R^2$  and low error values. The pseudo-first order model describes the interaction of the sorbate with the adsorbent, where the adsorption rate is proportional to the number of vacant sites. This adsorption model only considers the interaction between the sites and sorbate, discarding the interaction between the adsorbed molecules. The concentration of active sites is considered constant, and the maximum adsorption corresponds to a single saturated monolayer of sorbate on the surface of the adsorbent [43]. The maximum predicted CO<sub>2</sub> uptake presented in Table 4 confirms the applicability of the pseudo-first order model to represent the CO<sub>2</sub> uptake for post-combustion conditions. Compared to the experimental uptake, the small differences have been reported before and could be related to the external resistance at the beginning of the adsorption [44].

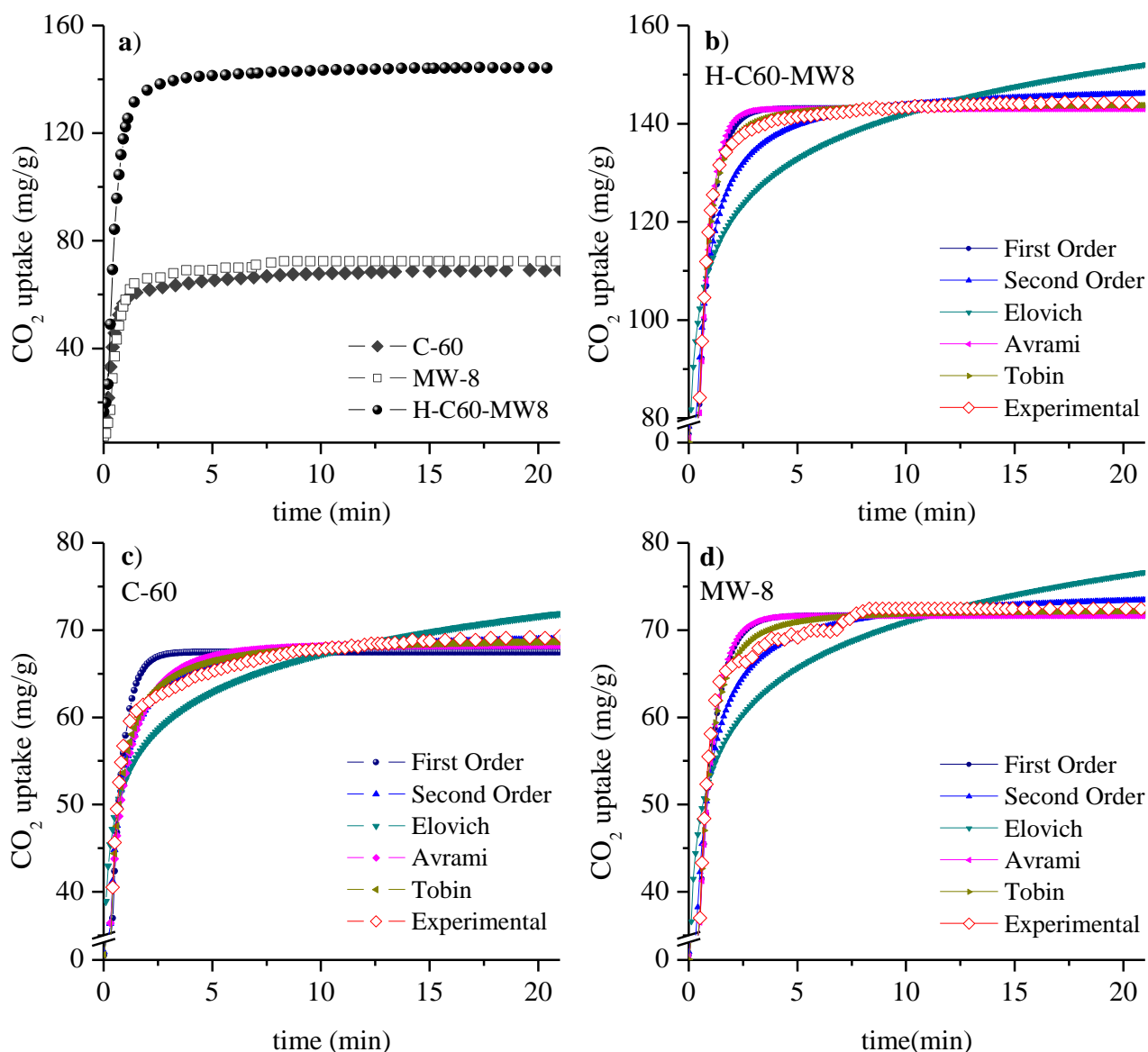


Fig. 8. Experimental and modelled adsorption kinetics. Thermogravimetric CO<sub>2</sub> adsorption at 1 bar and 25 °C.

Table 4. Kinetic data obtained by non-linear fitting analysis for selected activated carbons.

Model	Parameters	Sample		
		H-C60-MW8	MW-8	C-60
Pseudo-First order	$q_e, \text{mg}\cdot\text{g}^{-1}$	143.20	71.69	67.48
	$k_1, \text{min}^{-1}$	1.691	1.410	1.936
	$R^2$	0.999	0.999	0.928
	$E, \%$	$1.73\pm 7.2$	$1.66\pm 7.40$	$2.87\pm 5.97$

Pseudo-Second order	$q_e, \text{mg} \cdot \text{g}^{-1}$	148.35	74.85	69.89
	$k_2, \text{g} \cdot \text{mg}^{-1} \cdot \text{min}^{-1}$	0.022	0.034	0.050
	$R^2$	0.935	0.946	0.977
	$E, \%$	$3.09 \pm 12.19$	$3.163 \pm 12.71$	$1.45 \pm 6.28$
Tobin	$q_e, \text{mg} \cdot \text{g}^{-1}$	143.85	72.30	69.26
	$k_t$	4.964	3.315	3.816
	$n_T$	1.855	1.702	1.128
	$R^2$	0.993	0.986	0.979
	$E, \%$	$1.15 \pm 7.35$	$1.83 \pm 7.33$	$1.55 \pm 6.13$
Avrami	$q_e, \text{mg} \cdot \text{g}^{-1}$	143.03	71.65	68.28
	$k_A, \text{min}^{-1}$	1.674	1.409	2.042
	$N_A$	1.125	1.045	0.593
	$R^2$	0.985	0.969	0.957
	$E, \%$	$1.60 \pm 6.77$	$2.63 \pm 7.10$	$2.11 \pm 5.77$
Elovich	$\alpha, \text{mg} \cdot \text{g}^{-1} \cdot \text{min}^{-1}$	55070.0	8092.1	27850.0
	$\beta, \text{g} \cdot \text{mg}^{-1}$	0.075	0.131	0.159
	$R^2$	0.650	0.713	0.789
	$E, \%$	$8.25 \pm 30.22$	$8.69 \pm 31.27$	$4.94 \pm 16.72$

### 3.4 Adsorbent stability and recyclability

Adsorbent stability and recyclability were evaluated after several adsorption-desorption cycles at 1 bar and 25 °C using 100 % CO<sub>2</sub> in a thermogravimetric analyser. Fig. 9 showed the adsorbent H-C60-MW8 has an extraordinary recyclability nature, preserving up to 99% of the CO<sub>2</sub> uptake after 16 cycles. This result is in agreement with the fast adsorption equilibrium, and complete desorption can be attained in less than 15 min. The high stability and recyclability suggest that the mechanism governing the CO<sub>2</sub> uptake is physisorption.



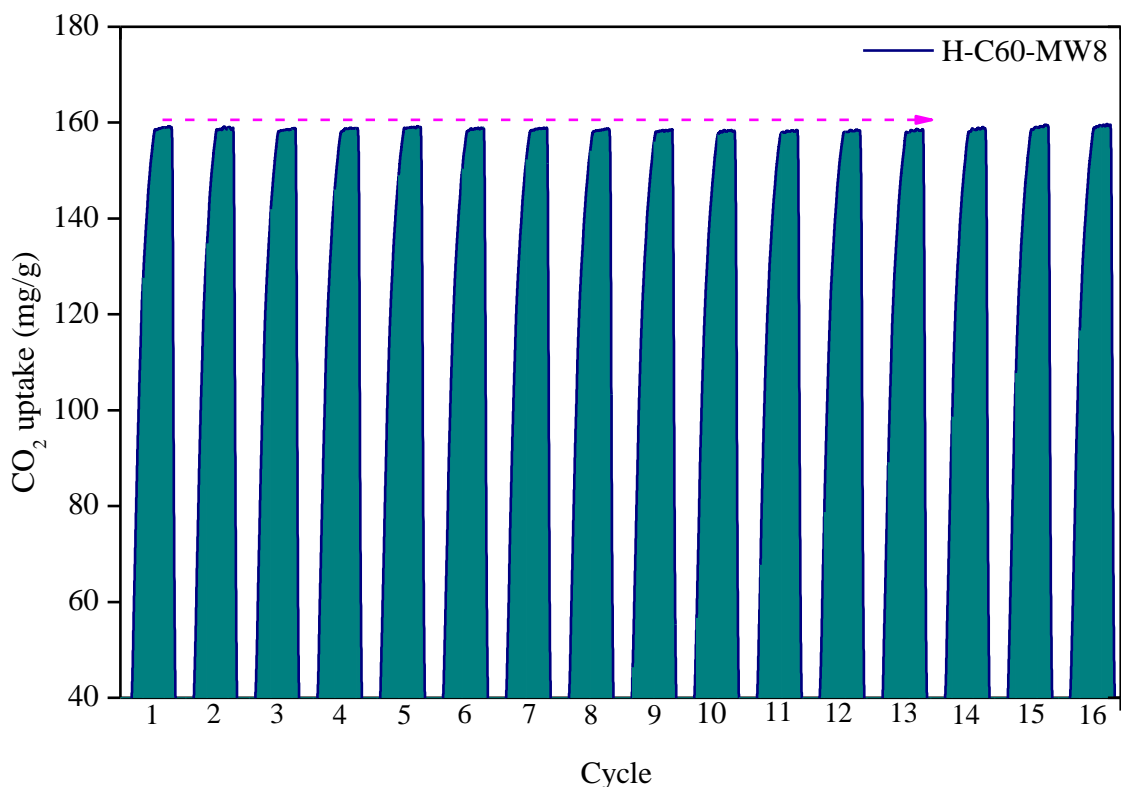


Fig. 9. Cyclic CO<sub>2</sub> adsorption performance of H-C60-MW8 activated carbon. Thermogravimetric CO<sub>2</sub> adsorption at 1 bar and 25°C.

The CO<sub>2</sub> adsorption profiles at 0 °C in a fresh and after 16 adsorption-desorption cycles on a H-C60-MW8 sample are shown in Fig. S2 (Supplementary information). It can be observed that, after 16 cycles, the sample has similar CO<sub>2</sub> uptake performance compared to the fresh activated carbon. This could be explained as result the textural properties, where it is evident that the sample maintain similar textural parameters. (See Fig. S3 and Table S2) (Supplementary information).

In order to evaluate the possible commercial application of hybrid activated carbon H-C60-MW8 in post-combustion capture, the CO<sub>2</sub> uptake was explored in the range of temperatures 25 – 60 °C and 15% CO<sub>2</sub> at 1 bar and the results are shown in Fig. S4 (Supplementary information). As expected, the CO<sub>2</sub> uptake decreased at higher temperatures as the CO<sub>2</sub> has a higher molecular kinetic energy, which allows CO<sub>2</sub> to escape form the adsorbent. At 15 % CO<sub>2</sub>,

the sample H-C60-MW6 absorbed 58.3, 47.4 and 25.3 mg g<sup>-1</sup> at 25, 35 and 65 °C, respectively. The values are comparable to the values reported previously in literature [45].

## 4 Conclusions

In the present study, hybrid activated carbons were prepared for the first time by coupling both conventional and microwave heating, and compared systematically to the individual heating technologies. The results confirmed synergic effects and the significant reduction of processing time to produce unique and competitive carbon adsorbents with a large volume of micropores and enhanced CO<sub>2</sub> uptake properties for post-combustion applications. The outstanding improvement in textural properties of H-C60-MW8 ( $S_{\text{BET}}$  area 100 & 57% higher than C-60 and MW-8) and CO<sub>2</sub> uptake (80 & 57% higher than C-60 and MW-8) proved the potential of using hybrid heating technologies, and establishes the basis for the future research and optimisation in the synthesis of engineered porous materials. The hybrid activated carbon prepared at a low impregnation ratio and by the combination of mild temperature and microwave conditions, showed excellent CO<sub>2</sub> uptake capacities and the potential for the optimisation of the parameters for the large-scale synthesis in environmental applications.

### Conflicts of interest

There are no conflicts to declare.

### Acknowledgements

The authors are grateful for the support of Matthew Nicholls.

### References

- [1] F.M. Kasperiski, E.C. Lima, C.S. Umpierres, G.S. dos Reis, P.S. Thue, D.R. Lima, S.L.P. Dias, C. Saucier, J.B. da Costa, Production of porous activated carbons from *Caesalpinia ferrea* seed pod wastes: Highly efficient removal of captopril from aqueous solutions, *J. Clean. Prod.* 197 (2018) 919–929. <https://doi.org/10.1016/j.jclepro.2018.06.146>.

- [2] G. Durán-Jiménez, V. Hernández-Montoya, M.A. Montes-Morán, S.W. Kingman, T. Monti, E.R. Binner, Microwave pyrolysis of pecan nut shell and thermogravimetric, textural and spectroscopic characterization of carbonaceous products, *J. Anal. Appl. Pyrolysis*. 135 (2018) 160–168. <https://doi.org/10.1016/j.jaap.2018.09.007>.
- [3] M. Danish, T. Ahmad, A review on utilization of wood biomass as a sustainable precursor for activated carbon production and application, *Renew. Sustain. Energy Rev.* 87 (2018) 1–21. <https://doi.org/10.1016/j.rser.2018.02.003>.
- [4] W. Sangchoom, R. Mokaya, Valorization of Lignin Waste: Carbons from Hydrothermal Carbonization of Renewable Lignin as Superior Sorbents for CO<sub>2</sub> and Hydrogen Storage, *ACS Sustain. Chem. Eng.* 3 (2015) 1658–1667. <https://doi.org/10.1021/acssuschemeng.5b00351>.
- [5] B. Li, Y. Cheng, L. Dong, Y. Wang, J. Chen, C. Huang, D. Wei, Y. Feng, D. Jia, Y. Zhou, Nitrogen doped and hierarchically porous carbons derived from chitosan hydrogel via rapid microwave carbonization for high-performance supercapacitors, *Carbon N. Y.* 122 (2017) 592–603. <https://doi.org/10.1016/j.carbon.2017.07.009>.
- [6] H. Deng, L. Yang, G. Tao, J. Dai, Preparation and characterization of activated carbon from cotton stalk by microwave assisted chemical activation-Application in methylene blue adsorption from aqueous solution, *J. Hazard. Mater.* 166 (2009) 1514–1521. <https://doi.org/10.1016/j.jhazmat.2008.12.080>.
- [7] Z. Emami, S. Azizian, Preparation of activated carbon from date sphate using microwave irradiation and investigation of its capability for removal of dye pollutant from aqueous media, *J. Anal. Appl. Pyrolysis*. 108 (2014) 176–184. <https://doi.org/10.1016/j.jaap.2014.05.002>.
- [8] E.T. Kostas, G. Durán-Jiménez, B.J. Shepherd, W. Meredith, L.A. Stevens, O.S.A. Williams, G.J. Lye, J.P. Robinson, Microwave pyrolysis of olive pomace for bio-oil and bio-char production, *Chem. Eng. J.* 387 (2020) 123404. <https://doi.org/10.1016/j.cej.2019.123404>.
- [9] G. Durán-Jiménez, V. Hernández-Montoya, M.A. Montes-Morán, M. Teutli-León, New oxygenated carbonaceous adsorbents prepared by combined radiant/microwave heating for the removal of Pb<sup>2+</sup> in aqueous solution, *J. Anal. Appl. Pyrolysis*. 113 (2015) 599–605. <https://doi.org/10.1016/j.jaap.2015.04.001>.
- [10] G. Durán-Jiménez, L.A. Stevens, G.R. Hodgins, J. Uguna, J. Ryan, E.R. Binner, J.P. Robinson, Fast regeneration of activated carbons saturated with textile dyes: Textural, thermal and dielectric characterization, *Chem. Eng. J.* 378 (2019) 121774. <https://doi.org/10.1016/j.cej.2019.05.135>.
- [11] F.C. Borges, Z. Du, Q. Xie, J.O. Trierweiler, Y. Cheng, Y. Wan, Y. Liu, R. Zhu, X. Lin, P. Chen, R. Ruan, Fast microwave assisted pyrolysis of biomass using microwave absorbent, *Bioresour. Technol.* 156 (2014) 267–274.

<https://doi.org/10.1016/j.biortech.2014.01.038>.

- [12] A. Soni, J. Smith, A. Thompson, G. Brightwell, Microwave-induced thermal sterilization- A review on history, technical progress, advantages and challenges as compared to the conventional methods, *Trends Food Sci. Technol.* 97 (2020) 433–442. <https://doi.org/10.1016/j.tifs.2020.01.030>.
- [13] J.P. Barham, E. Koyama, Y. Norikane, N. Ohneda, T. Yoshimura, Microwave Flow: A Perspective on Reactor and Microwave Configurations and the Emergence of Tunable Single-Mode Heating Toward Large-Scale Applications, *Chem. Rec.* 19 (2019) 188–203. <https://doi.org/10.1002/tcr.201800104>.
- [14] R. Hoseinzadeh Hesas, W.M.A. Wan Daud, J.N. Sahu, A. Arami-Niya, The effects of a microwave heating method on the production of activated carbon from agricultural waste: A review, *J. Anal. Appl. Pyrolysis.* 100 (2013) 1–11. <https://doi.org/10.1016/j.jaap.2012.12.019>.
- [15] J. Sun, W. Wang, Q. Yue, Review on microwave-matter interaction fundamentals and efficient microwave-associated heating strategies, *Materials (Basel).* 9 (2016). <https://doi.org/10.3390/ma9040231>.
- [16] O. Baytar, Ö. Şahin, C. Saka, Sequential application of microwave and conventional heating methods for preparation of activated carbon from biomass and its methylene blue adsorption, *Appl. Therm. Eng.* 138 (2018) 542–551. <https://doi.org/10.1016/j.applthermaleng.2018.04.039>.
- [17] W. Ao, J. Fu, X. Mao, Q. Kang, C. Ran, Y. Liu, H. Zhang, Z. Gao, J. Li, G. Liu, J. Dai, Microwave assisted preparation of activated carbon from biomass: A review, *Renew. Sustain. Energy Rev.* 92 (2018) 958–979. <https://doi.org/10.1016/j.rser.2018.04.051>.
- [18] G.K. Parshetti, S. Chowdhury, R. Balasubramanian, Biomass derived low-cost microporous adsorbents for efficient CO<sub>2</sub> capture, *Fuel.* 148 (2015) 246–254. <https://doi.org/10.1016/j.fuel.2015.01.032>.
- [19] C. Zhang, W. Song, Q. Ma, L. Xie, X. Zhang, H. Guo, Enhancement of CO<sub>2</sub> Capture on Biomass-Based Carbon from Black Locust by KOH Activation and Ammonia Modification, *Energy and Fuels.* 30 (2016) 4181–4190. <https://doi.org/10.1021/acs.energyfuels.5b02764>.
- [20] M.N. Anwar, A. Fayyaz, N.F. Sohail, M.F. Khokhar, M. Baqar, W.D. Khan, K. Rasool, M. Rehan, A.S. Nizami, CO<sub>2</sub> capture and storage: A way forward for sustainable environment, *J. Environ. Manage.* 226 (2018) 131–144. <https://doi.org/10.1016/j.jenvman.2018.08.009>.
- [21] M. Li, R. Xiao, Preparation of a dual Pore Structure Activated Carbon from Rice Husk Char as an Adsorbent for CO<sub>2</sub> Capture, *Fuel Process. Technol.* 186 (2019) 35–39.

<https://doi.org/10.1016/j.fuproc.2018.12.015>.

- [22] T. Watari, B.C. McLellan, D. Giurco, E. Dominish, E. Yamasue, K. Nansai, Total material requirement for the global energy transition to 2050: A focus on transport and electricity, *Resour. Conserv. Recycl.* 148 (2019) 91–103. <https://doi.org/10.1016/j.resconrec.2019.05.015>.
- [23] D. Gielen, F. Boshell, D. Saygin, M.D. Bazilian, N. Wagner, R. Gorini, The role of renewable energy in the global energy transformation, *Energy Strateg. Rev.* 24 (2019) 38–50. <https://doi.org/10.1016/j.esr.2019.01.006>.
- [24] G. Durán-Jiménez, L.A. Stevens, E.T. Kostas, V. Hernández-Montoya, J.P. Robinson, E.R. Binner, Rapid, simple and sustainable synthesis of ultra-microporous carbons with high performance for CO<sub>2</sub> uptake, via microwave heating, *Chem. Eng. J.* 388 (2020) 124309. <https://doi.org/10.1016/j.cej.2020.124309>.
- [25] G. Duran-Jimenez, T. Monti, J.J. Titman, V. Hernandez-Montoya, S.W. Kingman, E.R. Binner, New insights into microwave pyrolysis of biomass: Preparation of carbon-based products from pecan nutshells and their application in wastewater treatment, *J. Anal. Appl. Pyrolysis.* 124 (2017) 113–121. <https://doi.org/10.1016/j.jaap.2017.02.013>.
- [26] M. Thommes, K. Kaneko, A. V. Neimark, J.P. Olivier, F. Rodriguez-Reinoso, J. Rouquerol, K.S.W. Sing, Physisorption of gases, with special reference to the evaluation of surface area and pore size distribution (IUPAC Technical Report), *Pure Appl. Chem.* 87 (2015) 1051–1069. <https://doi.org/10.1515/pac-2014-1117>.
- [27] G. Durán-Jiménez, V. Hernández-Montoya, M.A. Montes-Morán, A. Bonilla-Petriciolet, N.A. Rangel-Vázquez, Adsorption of dyes with different molecular properties on activated carbons prepared from lignocellulosic wastes by Taguchi method, *Microporous Mesoporous Mater.* 199 (2014) 99–107. <https://doi.org/10.1016/j.micromeso.2014.08.013>.
- [28] X. Liu, Y. Sun, J. Liu, C. Sun, H. Liu, Q. Xue, E. Smith, C. Snape, Potassium and Zeolitic Structure Modified Ultra-microporous Adsorbent Materials from a Renewable Feedstock with Favorable Surface Chemistry for CO<sub>2</sub> Capture, *ACS Appl. Mater. Interfaces.* 9 (2017) 26826–26839. <https://doi.org/10.1021/acsami.7b06665>.
- [29] P. González-García, Activated carbon from lignocellulosics precursors: A review of the synthesis methods, characterization techniques and applications, *Renew. Sustain. Energy Rev.* 82 (2018) 1393–1414. <https://doi.org/10.1016/j.rser.2017.04.117>.
- [30] H. Yang, Y. Yuan, S.C.E. Tsang, Nitrogen-enriched carbonaceous materials with hierarchical micro-mesopore structures for efficient CO<sub>2</sub> capture, *Chem. Eng. J.* 185–186 (2012) 374–379. <https://doi.org/10.1016/j.cej.2012.01.083>.
- [31] M.L. Botomé, P. Poletto, J. Junges, D. Perondi, A. Dettmer, M. Godinho, Preparation

- and characterization of a metal-rich activated carbon from CCA-treated wood for CO<sub>2</sub> capture, *Chem. Eng. J.* 321 (2017) 614–621. <https://doi.org/10.1016/j.cej.2017.04.004>.
- [32] A.E. Ogungbenro, D. V. Quang, K.A. Al-Ali, L.F. Vega, M.R.M. Abu-Zahra, Physical synthesis and characterization of activated carbon from date seeds for CO<sub>2</sub> capture, *J. Environ. Chem. Eng.* 6 (2018) 4245–4252. <https://doi.org/10.1016/j.jece.2018.06.030>.
- [33] S. Deng, H. Wei, T. Chen, B. Wang, J. Huang, G. Yu, Superior CO<sub>2</sub> adsorption on pine nut shell-derived activated carbons and the effective micropores at different temperatures, *Chem. Eng. J.* 253 (2014) 46–54. <https://doi.org/10.1016/j.cej.2014.04.115>.
- [34] S.W. Choi, J. Tang, V.G. Pol, K.B. Lee, Pollen-derived porous carbon by KOH activation: Effect of physicochemical structure on CO<sub>2</sub> adsorption, *J. CO<sub>2</sub> Util.* 29 (2019) 146–155. <https://doi.org/10.1016/j.jcou.2018.12.005>.
- [35] J. Li, B. Michalkiewicz, J. Min, C. Ma, X. Chen, J. Gong, E. Mijowska, T. Tang, Selective preparation of biomass-derived porous carbon with controllable pore sizes toward highly efficient CO<sub>2</sub> capture, *Chem. Eng. J.* 360 (2019) 250–259. <https://doi.org/10.1016/j.cej.2018.11.204>.
- [36] S.Y. Lee, H.M. Yoo, S.W. Park, S. Hee Park, Y.S. Oh, K.Y. Rhee, S.J. Park, Preparation and characterization of pitch-based nanoporous carbons for improving CO<sub>2</sub> capture, *J. Solid State Chem.* 215 (2014) 201–205. <https://doi.org/10.1016/j.jssc.2014.03.038>.
- [37] G. Durán-Jiménez, E.T. Kostas, L.A. Stevens, W. Meredith, M. Erans, V. Hernández-Montoya, A. Buttress, C.N. Uguna, E. Binner, Green and simple approach for low-cost bioproducts preparation and CO<sub>2</sub> capture, *Chemosphere.* 279 (2021). <https://doi.org/10.1016/j.chemosphere.2021.130512>.
- [38] Z. Zhang, D. Luo, G. Lui, G. Li, G. Jiang, Z.P. Cano, Y.P. Deng, X. Du, S. Yin, Y. Chen, M. Zhang, Z. Yan, Z. Chen, In-situ ion-activated carbon nanospheres with tunable ultramicroporosity for superior CO<sub>2</sub> capture, *Carbon N. Y.* 143 (2019) 531–541. <https://doi.org/10.1016/j.carbon.2018.10.096>.
- [39] C. Chen, H. Huang, Y. Yu, J. Shi, C. He, R. Albilali, H. Pan, Template-free synthesis of hierarchical porous carbon with controlled morphology for CO<sub>2</sub> efficient capture, *Chem. Eng. J.* 353 (2018) 584–594. <https://doi.org/10.1016/j.cej.2018.07.161>.
- [40] S.H. Hsu, C.S. Huang, T.W. Chung, S. Gao, Adsorption of chlorinated volatile organic compounds using activated carbon made from *Jatropha curcas* seeds, *J. Taiwan Inst. Chem. Eng.* 45 (2014) 2526–2530. <https://doi.org/10.1016/j.jtice.2014.05.028>.
- [41] P. Lahijani, M. Mohammadi, A.R. Mohamed, Metal incorporated biochar as a potential adsorbent for high capacity CO<sub>2</sub> capture at ambient condition, *J. CO<sub>2</sub> Util.* 26 (2018) 281–293. <https://doi.org/10.1016/j.jcou.2018.05.018>.

- [42] J. Serafin, M. Baca, M. Biegun, E. Mijowska, R.J. Kaleńczuk, J. Sreńscek-Nazzal, B. Michalkiewicz, Direct conversion of biomass to nanoporous activated biocarbons for high CO<sub>2</sub> adsorption and supercapacitor applications, *Appl. Surf. Sci.* 497 (2019). <https://doi.org/10.1016/j.apsusc.2019.143722>.
- [43] L. Largitte, R. Pasquier, A review of the kinetics adsorption models and their application to the adsorption of lead by an activated carbon, *Chem. Eng. Res. Des.* 109 (2016) 495–504. <https://doi.org/10.1016/j.cherd.2016.02.006>.
- [44] S. Jribi, T. Miyazaki, B.B. Saha, A. Pal, M.M. Younes, S. Koyama, A. Maalej, Equilibrium and kinetics of CO<sub>2</sub> adsorption onto activated carbon, *Int. J. Heat Mass Transf.* 108 (2017) 1941–1946. <https://doi.org/10.1016/j.ijheatmasstransfer.2016.12.114>.
- [45] G. Srinivas, V. Krungleviciute, Z.X. Guo, T. Yildirim, Exceptional CO<sub>2</sub> capture in a hierarchically porous carbon with simultaneous high surface area and pore volume, *Energy Environ. Sci.* 7 (2014) 335–342. <https://doi.org/10.1039/c3ee42918k>.